



Orbital Debris Quarterly News

Volume 18, Issue 2
April 2014

Inside...

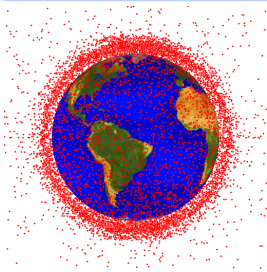
**Nicholas Johnson
Retires as NASA Chief
Scientist for OD.....2**

**First Results of
WFPC2 Crater
Analysis Presented
at 2014 LPSC.....2**

**NASA MCAT's
New Destination is
Ascension Island.....4**

**Hypervelocity Impact
Test with Large Mass
Projectile.....6**

**Space Missions
and Satellite
Box Score.....9**



A publication of
the NASA Orbital
Debris Program Office

International Space Station Maneuvers Twice to Avoid Tracked Debris

After more than a year without a collision avoidance maneuver, the International Space Station (ISS) recently performed two maneuvers to avoid conjunctions with two separate debris pieces. The first maneuver was implemented at 1:30 GMT on 17 March against tracked debris (International Designator 1979-095B], U.S. Space Surveillance Network [SSN] satellite number 36917). This was the 17th ISS collision avoidance maneuver since 1999, but the first since 31 October 2012. The debris was a small, high drag object that originated from the Meteor 2-5 spacecraft (International Designator 1979-095A, U.S. SSN number 11605). Meteor 2-5 was a Soviet meteorological satellite that was launched into an 880 km x 865 km, 81.2° inclination orbit on 31 October 1979. The satellite has experienced multiple debris release events since that time, and 36917 was one of those

catalogued by the U.S. Space Surveillance Network.

The second maneuver (18th in ISS history) occurred on 3 April at 20:42 GMT. The predicted conjunction was against mission-related debris from an Ariane 5 launch (International Designator 2009-044D, U.S. SSN number 35758). The debris was a SYLDA (SYstème de Lancement Double Ariane) used to launch two satellites on an Ariane 5. This object was in a highly elliptical orbit (25,842 x 295 km) with an inclination of 2.5° and had a drag eight times greater than the ISS. Due to the high eccentricity and drag of the object, unusually large uncertainties were associated with its trajectory prediction. Although the final update prior to the maneuver indicated one was not needed, with the fluctuations in the SYLDA's orbit, a decision was made to perform the maneuver. ♦

NASA Resumes Haystack Data Collection

After more than a 3-year gap in coverage, the MIT Lincoln Laboratory Haystack radar has resumed collecting debris data for the NASA Orbital Debris Program Office (ODPO). The Haystack collects data on objects as small as 5 mm in the low Earth orbit (LEO) region. The radar's new name, reflecting its new capabilities, is the Haystack Ultra-wideband Satellite Imaging Radar (HUSIR). The ODPO mission does not use wide-band, and will continue to use an X-band continuous waveform, most often staring at 90° azimuth and 75° elevation. Approximately one-third of the time, the radar will stare at a south azimuth to collect data on debris with lower inclination orbits. Debris objects passing through



Radome cap lift in May 2010 was one of the first steps in the HUSIR integration sequence. The HUSIR has increased W-band resolution while maintaining X-band sensitivity.

continued on page 2

Haystack Data

continued from page 1

the beam are recorded when the signal-to-noise ratio (SNR) rises above a threshold. See ODQN, October 2013, p. 4 for more details on how the ODPO uses the data.

During the down period, the Haystack

Auxiliary Radar (HAX) collected additional hours of data to compensate for the loss of Haystack data. With its wider beam, HAX is useful in detecting larger, but still small, objects (approximately 2 cm and larger objects

in LEO). However, HAX cannot substitute for the sensitivity of the larger radar, and it is good to have Haystack, now HUSIR, back in full operation. ♦

Nicholas Johnson Retires as NASA Chief Scientist for Orbital Debris



Mr. Nicholas Johnson, NASA Chief Scientist for Orbital Debris since 1996, retired on March 28 after 43 years of government service and more than 35 years of working orbital debris issues. As Chief Scientist, Mr. Johnson served as the agency authority for orbital debris, including all aspects of

environment definition, present and future, and the operational and design implications of the environment to both manned and robotic space vehicles operating in Earth orbit. He was responsible for conceiving, conducting, and directing research to define the orbital debris environment, for determining operational techniques for spacecraft to protect themselves from the environment, and for recommending techniques to minimize the growth in the future orbital debris environment.

During his career, Mr. Johnson served in the Air Force as an aviation electronics technician and had one tour of duty in Vietnam. Later, as an officer in the U.S. Navy, Mr. Johnson was an instructor and served as Director of the Heat Transfer and Fluid Flow Division at the Navy's Nuclear Power School.

Mr. Johnson worked in industry from 1979 to 1996, first at Teledyne Brown Engineering and later at Kaman Sciences. He became an expert on space surveillance and the Soviet space program. He also worked on the Strategic Defense Initiative and the F-15 Anti-Satellite (ASAT) missile program. From these experiences, he became a strong advocate for limiting the growth of orbital debris.

After joining NASA, Mr. Johnson worked diligently to broaden and strengthen orbital debris mitigation guidelines and standards within NASA, the U.S. Government, and internationally. Due largely to Mr. Johnson's diligence, the U.S. Government Orbital Debris Mitigation Standard Practices were approved in 2001 and the Space Debris Mitigation Guidelines of the Committee on the Peaceful Uses of Outer Space (COPUOS) were adopted first by COPUOS and later by the full United Nations in 2007. Mr. Johnson led the U.S. delegation to the Inter-Agency Space Debris Coordination Committee (IADC) from 1996 to 2013.

Mr. Johnson is the author of several books including *Artificial Space Debris* with Darren McKnight and books on the Soviet space program. He has received many awards including the NASA Distinguished Service Medal, the NASA Exceptional Achievement Medal, and the Department of Defense's Joint Meritorious Civilian Service Award.

Mr. Johnson's many technical accomplishments and his ability to simultaneously bridge cultural and technical divides will be sorely missed. ♦

First Results of WFPC2 Crater Residue Analysis Presented at the 2014 LPSC

The annual Lunar and Planetary Science Conference (LPSC) brings together the world's experts in the planetary sciences, astronomy, geophysics, geochemistry, and geology to present their latest research results. The 45th LPSC was held 17-21 March 2014 at The Woodlands, Texas. Five posters describing the research and analysis efforts of the international NASA-European Space Agency team examining the Hubble Space Telescope

(HST) Wide Field Planetary Camera 2 (WFPC2) impact features and crater residues (Figure 1) were presented at Tuesday evening's *Presolar, Interplanetary and Cometary Dust* session. The posters, all bearing the titular prefix "Impacts on the Hubble Space Telescope Wide Field and Planetary Camera 2", examined Microanalysis and Recognition of Micrometeoroid Compositions (Kearsley *et al.*, abstract #1733), Ion Beam Analysis of Subtle Impact Features

(Colaix *et al.*, #1727), Smaller Particle Impacts (Ross *et al.*, #1514), Larger Particles (Kearsley *et al.*, #1722), and Experimental Simulation of Micrometeoroid Capture (Price *et al.*, #1466).

Kearsley *et al.* (#1733) describes the development of scanning electron microscope (SEM) energy dispersive X-ray (EDX) analysis techniques and protocols required to categorize impact crater residues as being of orbital

continued on page 3

WFPC2 Crater

continued from page 2

debris, micrometeoritic (MM), or unknown origins, though this poster, like all five, concentrates on the MM component. Despite the complex nature of the WFPC2 surface, carefully calibrated EDX spectra allow the team to ascertain the compositional signatures of impactors. Colaax *et al.* describe techniques developed at the University of Surrey's Ion Beam Centre, using ion beam analysis, to assess residue constituents for those craters found particularly challenging to SEM-EDX analysis. Proton-Induced X-ray Emission (PIXE) has demonstrated its superior ability to find and assess the signatures for very low concentration impact residues. The majority of impact features observed were small, not penetrating the WFPC2 thermal paint layer,

and Ross, *et al.* discusses the recognition, analysis, and interpretation of residues found in these smaller features. About 90% of these contained hypervelocity impact melt features, thus preserving information regarding the impactor's elemental constituents and origins. Figure 2 depicts one such crater and its elemental enrichment compared to the surface baseline composition; this crater displayed an excess of magnesium (Mg) and iron (Fe) but not aluminum (Al), leading to the conclusion that the trace element features are derived from the impactor and not the WFPC2 Al substrate. Kearsley *et al.* (#1722) describes the analysis of 63 larger impact features (> 700 μm size) and their residue materials. Price, *et al.* describes team efforts to simulate the impact of silicate

and sulfide minerals on WFPC2 analogues. Although conducted at lower velocities than expected for MM in LEO, the impact features and residue compositions closely match WFPC2 features. Their results validate the analytical methods presented in other posters for trace residue identification.

Taken as an ensemble, these posters represent the first presentation of the extensive analytical results generated by the international team's comprehensive analyses of the WFPC2 impact features. The reader is directed to the Universities Space Research Association's website, <http://www.hou.usra.edu/meetings/lpsc2014/pdf/ sess611.pdf>, for electronic access to these posters. ♦

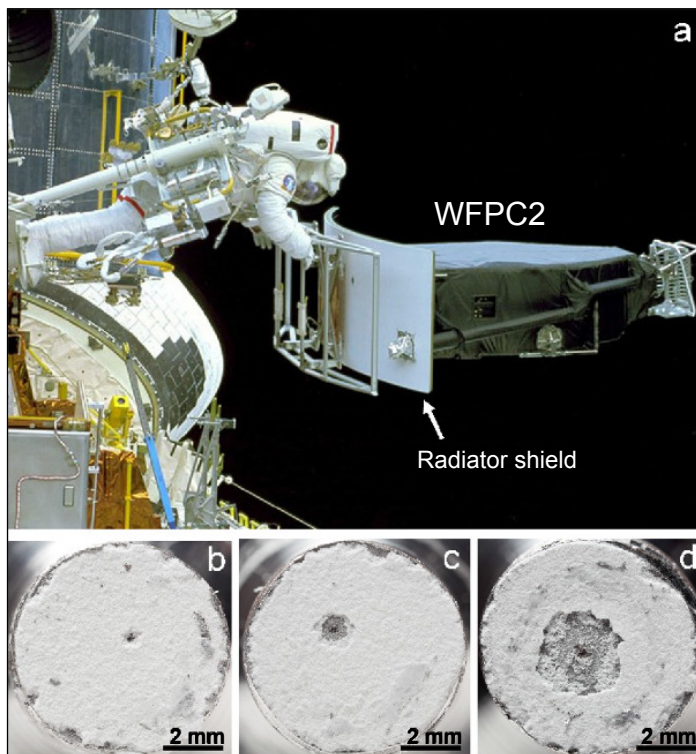


Figure 1. (Top) STS-125 astronaut stows WFPC2 after removing it from the HST. (Bottom) diverse features sizes in larger cores collected by NASA ODPO.

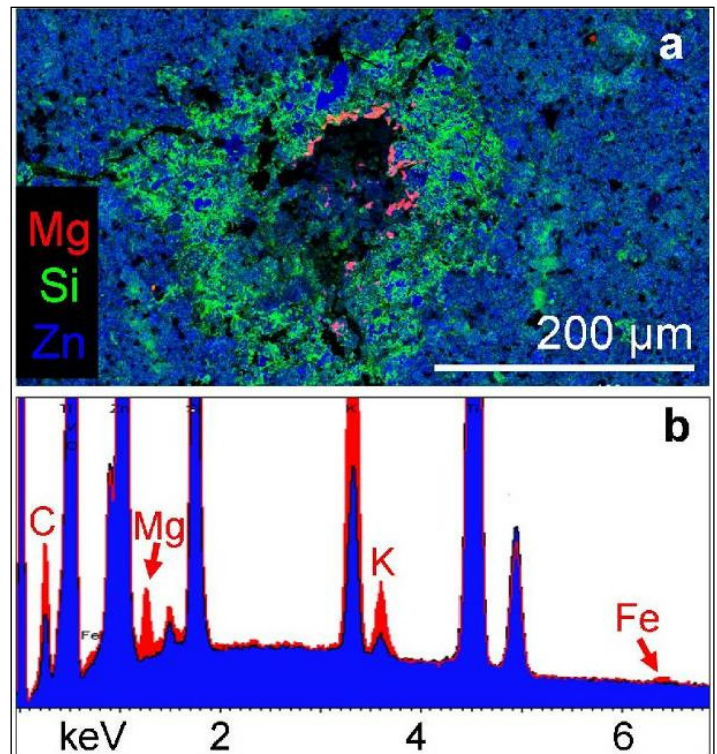


Figure 2: (Top) Elemental mapping for Mg, silicon (Si), and zinc (Zn) – the latter dominated by the thermal paint. (Bottom) SEM-EDX energy peaks, background or baseline in blue, excess due to residue in red.

UPDATE YOUR SUBSCRIPTION ADDRESS... If you have stopped receiving email notification when the latest ODQN is available, please update your email address using the ODQN Subscription Request Form located on the NASA Orbital Debris Program Office website, www.orbitaldebris.jsc.nasa.gov. This form can be accessed by clicking on "Quarterly News" in the Quick Links area of the website and selecting "ODQN Subscription" from the pop-up box that appears.

PROJECT REVIEW

The NASA Meter Class Autonomous Telescope's New Destination is Ascension Island

S. LEDERER

The Meter Class Autonomous Telescope (MCAT) will be the newest optical sensor dedicated to NASA's mission to characterize the space debris environment. It is the successor to a series of optical telescopes developed and operated by the NASA Orbital Debris Program Office (ODPO) to monitor and assess the debris environment in (1) low Earth orbit (LEO), (2) medium Earth orbit (MEO), and (3) Geosynchronous orbit (GEO), with emphasis on LEO and GEO altitudes. Construction will begin in fall 2014 with first light and operations expected in 2015.

A joint NASA – Air Force Research Lab project, MCAT is a 1.3 m telescope that will be dedicated to debris research utilizing optical wavelengths. Its optical path and sensor yield a large survey fence at the cutting edge of current detector performance. It will employ four primary operational observing modes, two

of which were not computationally feasible a decade ago. Operations will be supported by a sophisticated software suite that monitors clouds and weather conditions, and controls everything from data collection to dome rotation to processing tens of gigabytes of image data nightly. With fainter detection limits, precision detection, acquisition and tracking of targets, multi-color photometry, precision astrometry, automated re-acquisition capability, and the ability to process all data at the acquisition rate, MCAT is capable of producing and processing a volume and quality of data far in excess of any current (or prior) ODPO operations. This means higher fidelity population inputs and eliminating the multi-year backlog from acquisition-to-product typical of optical campaigns. All of this is possible given a suitable observing location.

Originally planned for the island of either Legan or Roi-Namur, part of the Kwajalein

Atoll Islands, recent developments have led to a change in venue for MCAT [1]. The Ground-based Electro-Optical Deep Space Surveillance, or GEODSS, system of ground-based telescopes is the United States' major tracking system for deep space (Figure 1). The additional Mòron Optical Space Surveillance (MOSS) telescope in Mòron, Spain (supplemental to the GEODSS system) closed recently, leaving a significant gap in ground-based longitudinal coverage between the Socorro, New Mexico and Diego Garcia sites. This longitudinal gap is well covered by placing a telescope on Ascension Island (7° 58' 20" S, 14° 24' 4" W), in the Atlantic Ocean.

The orbits of uncontrolled debris at GEO are known to oscillate between 0-15° inclination over a 50-year period. At nearly 8° S, Ascension Island is ideally suited to this task as the GEO belt sweeps across the zenith at this location, offering consistently favorable observational opportunities to access under-sampled low-inclination orbits and new GEO longitudes.

Ascension Island offers numerous additional advantages. As a British overseas territory with a U.S. Air Force base presence, the necessary infrastructure and support already exists. The MCAT will be deployed at the state-of-the-art secure Consolidated Instrumentation Facility (CIF) at an elevation of ~350' above sea level and roughly one mile from the ocean, eliminating direct exposure to sea-salt spray.

Constant trade winds from the SSE, originating from Africa, give promise to a steady laminar airflow over an island, a trait sought after to create stable atmospheric and good

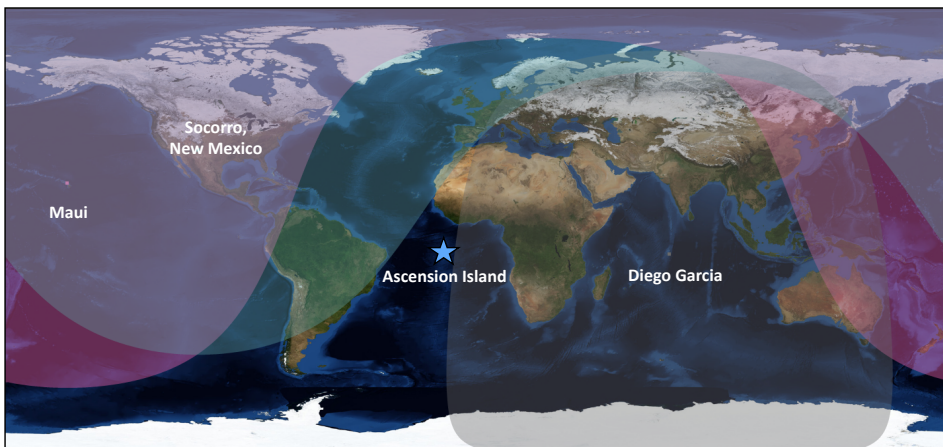


Figure 1. Ascension Island will fill a longitudinal gap not attainable by the current suite of GEODSS sensors.

continued on page 5

Monthly Availability at Ascension Island, Nighttime Only

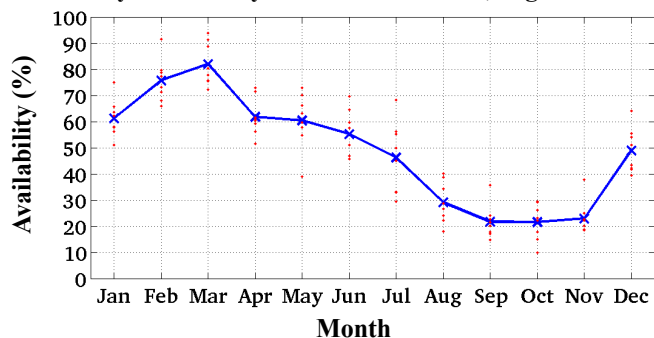


Figure 2. An estimate of the percentage of clear nights available as a function of time-of-year derived from Northrop Grumman Corporation's Meteosat Second Generation (MSG) over 8 years. Data are defined through a CFLOS analysis where clear is defined as an optical depth < 0.1 (the limit of the sensors). Red dots indicate the average for the indicated month for 1 year and the blue Xs indicate the average of 8 years (2005 – 2012) for that month.

Data were derived from Meteosat Second Generation (MSG) Imagery. Horizontal resolution is 4 km and temporal resolution is 30 minutes taken during the night (no daytime observations). Figure courtesy R. J. Alliss, Atmospheric Effects, Northrop Grumman Corporation.

MCAT

continued from page 4

astronomical ‘seeing’ conditions. Ascension boasts very low annual rainfall averages (7" of rain per year) and a fair (though not ideal) number of clear nights (Figure 2). Yearly cloud-free line of sight (CFLOS) measured between 2005 and 2012 ranged from ~ 40-55% clear skies. In addition, this low population island has strict lighting limitations due to a population of nesting sea turtles that require the darkest skies possible. This results in skies that are also ideal for an observatory.

This combination of attributes created the necessary compelling argument to redirect MCAT to its final destination: Ascension Island. As such, Ascension will provide a unique setting for an autonomous telescope dedicated to the NASA ODPO's goal of understanding the debris environment.

Instrumentation

Designed with a low latitude site and fast moving debris targets in mind, the 1.3 m f/4 DFM Engineering telescope can track LEO or GEO targets easily and smoothly through the zenith. The MCAT has the capability of tracking objects in LEO. Fast tracking with a telescope is only effective with an equally capable dome. The facility will be equipped with a 7-meter Observa-dome from the same manufacturer responsible for the domes erected by the GEODSS program, domes that have suffered no major down-time in 35 years. This high-speed tracking dome can rotate fast enough to track LEO objects.

A Spectral Instruments CCD optical camera will be attached to the telescope with two sets of broad-band photometric filters available for use in the 8-position DFM filter slide, including Sloan Digital Sky Survey (SDSS) g'r'i'z', and Johnson/Kron-Cousins BVRI filters (Figure 3). The large format CCD will have a $0.677^\circ \times 0.677^\circ$ (0.957° diagonal) field of view with $0.60''/\text{pix}$. With a fused silica window to allow UV/blue photons through the system, the optical wavelength range is $3000 \text{ \AA} - 1.06 \mu\text{m}$. The camera is a closed-loop Cryo-tiger cooling system (-100°C).

Operations

MCAT's primary goal is to characterize LEO, MEO and GEO orbital regimes statistically to better understand the debris environment by providing high fidelity data in a timely manner to protect satellites and spacecraft in orbit around the Earth. Toward

continued on page 6

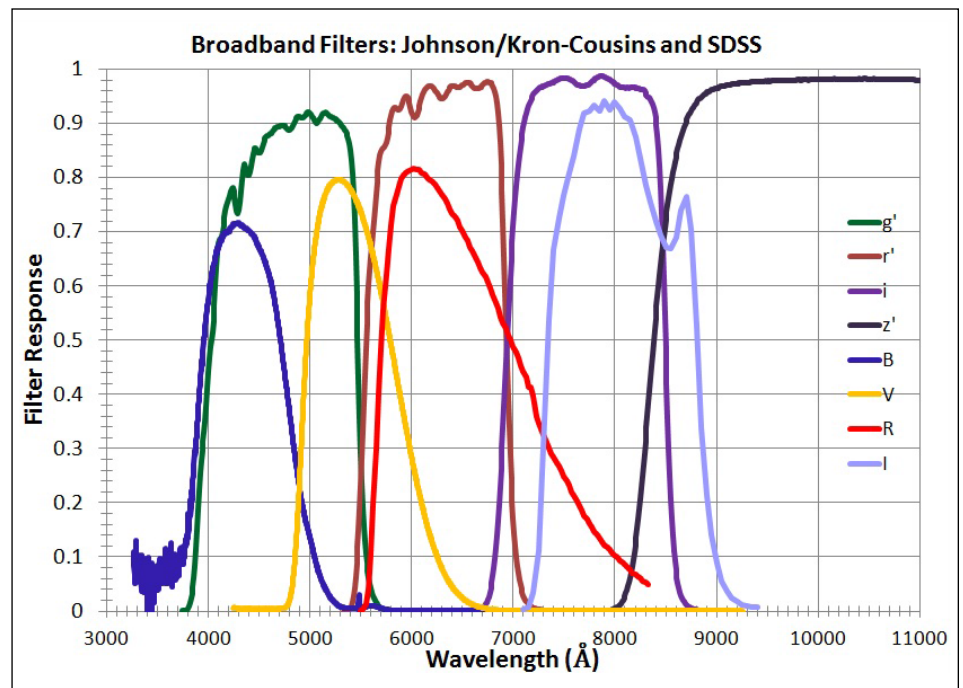


Figure 3. Plot of the filter response for Johnson and Kron-Cousins BVRI broadband filters and Sloan Digital Sky Survey (SDSS) g'r'i'z' filters.

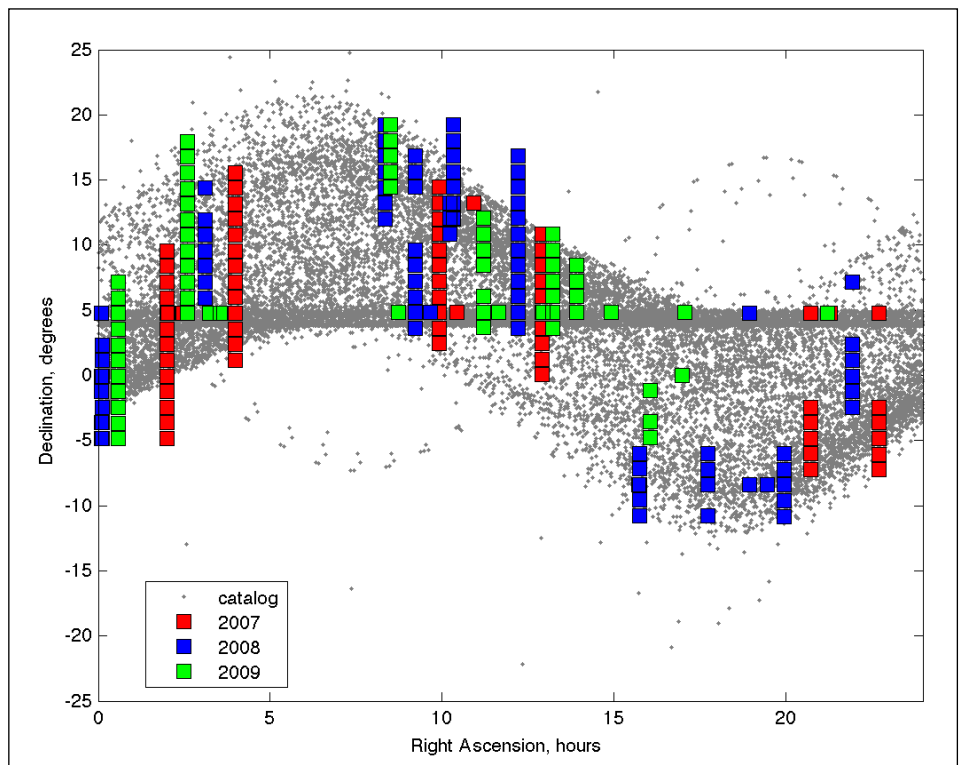


Figure 4. MODEST daily motion for GEO objects plotted as Declination versus Right Ascension; filled coverage map for years 2007-2009 as view from CTIO, Chile [2]. Note the GEO belt is centered at 5° Dec as viewed from CTIO. Grey dots indicate cataloged objects with mean motions $< 1.1 \text{ rev/day}$ and $\text{Inc} < 17^\circ$. MCAT will observe similar fields in its Counter-sidereal TDI or GEO stare and chase operational modes.

MCAT

continued from page 5

this end, a fully automated software package has been designed specifically for MCAT by Euclid Research of Canada to command the telescope and dome, monitor weather and clouds, determine the priority of observing, collect data, and (during the following daytime hours), perform a standardized data reduction procedure. This 'reduced' data will then be sent via satellite to NASA ODPO for analysis.

MCAT's unique capabilities include four sophisticated observing modes that involve automated detection, acquisition, tracking, and – via preliminary orbit generation and refinement – re-acquisition of both GEO and LEO targets. They include: (1) GEO survey/GEO follow-up mode, (2) Catalog/Object of Interest mode, (3) Orbit Scan mode (LEO), and (4) Stare-Detect-Chase mode (LEO). Figure 4 shows the expected field mapping of the GEO field at a snapshot in time (GEO survey). The Catalog/Object of Interest mode tracks a known target with known orbital parameters. The newer Orbit Scan mode tracks an expected orbital rate to detect unknown objects. Stare-Detect-Chase mode detects streaks, and in real-time, calculates the expected orbital rate and direction to chase the newly detected object. In the event of an explosion or collision, MCAT affords NASA the ability to rapidly respond to the event and track the time evolution

of the cloud of debris. For all modes, filter photometry will be employed to characterize targets (e.g., brightness measurements can be used to estimate sizes or lightcurves for rotation/tumble rates).

Other global sensors may also hand-off targets to MCAT for better overall orbit determination. Through its unique longitude, MCAT can be used to support Space Situational Awareness (SSA) and the Space Surveillance Network (SSN) by providing astrometry, catalog maintenance, or catalog metrics data to U.S. Strategic Command (USSTRATCOM) or the Joint Space Operations Center (JSpOC). Here, the unique longitude of Ascension becomes a true asset. Combining this information with range to the target, one might also gain insight into the shape of the target to give intrinsic insight into the risks posed to GEO spacecraft by the object.

Summary

NASA's MCAT has the potential to improve NASA's understanding of the debris environment significantly, which is essential to ensuring the safety of all spacecraft in orbit around the Earth. The new destination of Ascension Island offers a variety of benefits. The unique latitude/longitude will fill a significant gap in the GEODSS network's coverage of

the sky. From an astronomical perspective, the environment is promising with limited rainfall, steady trade-winds producing laminar flow over the island, potentially stable 'seeing' conditions, and dark skies. Personnel and infrastructure support at this remote location will be critical for the success of an automated telescope. To accomplish its goals, MCAT will employ four major operational modes. All this is made possible due to the marriage of sophisticated automated software, a suite of weather sensors, advanced instrumentation, a fast tracking telescope and dome, and a very dedicated team of engineers and scientists.

For further information, see Lederer, et al. [3].

References

1. Stansbery, E.G., et al. Meter-Class Autonomous Telescope for Space Debris Research, 2003 *AMOS Technical Conference Proceedings*, 2003.
2. Abercromby K.J., et al. Michigan Orbital Debris Survey Telescope (MODEST) Observations of the Geosynchronous Orbital Debris Environment Observing Years: 2007-2009, NASA TP-2011-217350, 2011.
3. Lederer, S.L., et al. The NASA Meter Class Autonomous Telescope: Ascension Island. *AMOS Technical Conference Proceedings*, 2013. ♦

Hypervelocity Impact Test with Large Mass Projectile

E. CHRISTIANSEN, A. DAVIS,
J. MILLER, AND D. LEAR

A hypervelocity impact test was conducted with a 598 g projectile at 6.905 km/s on a

NASA supplied multi-shock shield. The projectile was a hollow aluminum and nylon cylinder with an outside diameter of 8.6 cm and length of 10.3 cm. This test was performed

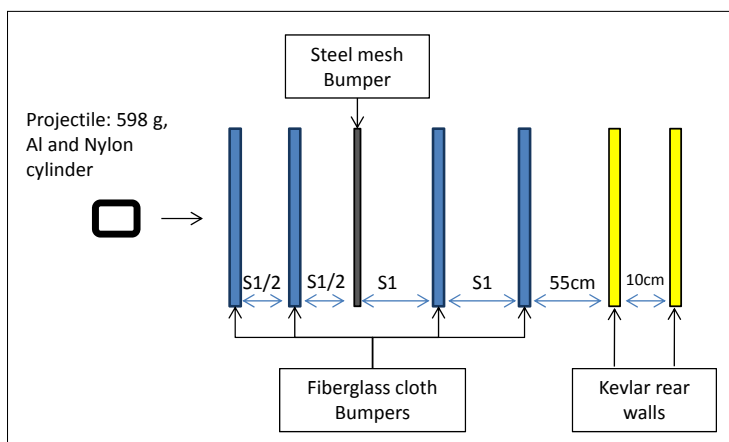


Figure 1. Diagram of multi-shock shield target.

in February 2014 at Arnold Engineering Development Complex (AEDC) in preparation for the Debrisat test in April 2014. This piggy-back opportunity was generously provided by the AEDC Range Team. Figure 1 illustrates the multi-

shock shield test article, which consisted of five separate bumpers, four of which were fiberglass fabric and one of steel mesh, and two rear walls, each consisting of Kevlar fabric. The overall length of the test article was 2.65 m. Figure 2 shows the test article after loading on a truck prior to shipping to AEDC. The test article was a 5X scaled-up version of a smaller multi-shock shield previously tested using a 1.4 cm diameter aluminum projectile for an inflatable module project several years ago. Hydrocode simulations were performed prior to the impact test and indicated that some adjustments were needed to the shield to successfully stop the projectile in the AEDC test, primarily because the cylindrical shape was difficult to fragment. Therefore, a steel mesh bumper was added

continued on page 7

Hypervelocity

continued from page 6

to the shield configuration to induce greater fragmentation of the projectile. Figure 3 illustrates the results of a hydrocode simulation indicating that shield penetration would occur without the steel mesh.

The AEDC test occurred as planned, and the NASA multi-shock shield was successful

at stopping the 598 g projectile (Figures 4 to 5). The fifth bumper layer was not completely penetrated, although it was torn free from its support structure and thrown into the first rear wall. The outer Kevlar layer of the first rear wall was torn (probably from the frame of the fifth bumper layer that impacted into the rear

wall), but the back of the rear wall was intact (Figure 6). No damage occurred to the second rear wall, or to the witness plate behind the target. The table below indicates the damage to each layer of the shield. The data from this test will be used in updating the multi-shock shield ballistic limit equations. ♦



Figure 2. Pre-test image of multi-shock shield target. First fiberglass bumper is on right, Kevlar rear walls are on left.

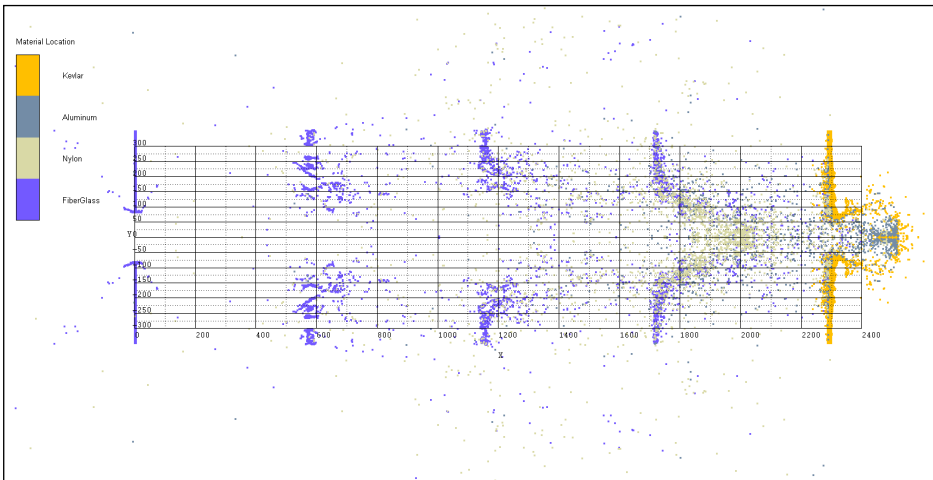


Figure 3. Hydrocode simulation of multi-shock shield without steel mesh included. Impact direction left to right. Shield rear wall failed (on right).



Figure 4. Post-test image of multi-shock shield target. First fiberglass bumper on right, Kevlar rear walls on left.



Figure 5. Post-test image of multi-shock shield. Front view of target.



Figure 6. Post-test image of multi-shock shield. Kevlar rear walls are intact (no complete penetration).

Table 1. Multi-shock Shield Damage Measurements.

Bumper 1: Fiberglass	Bumper 2: Fiberglass	Bumper 3: steel mesh	Bumper 4: Fiberglass	Bumper 5: Fiberglass	Rear wall 1: Kevlar	Rear wall 2: Kevlar
130 mm diameter perforation	300 mm diameter perforation	600 mm diameter perforation	300 mm diameter perforation (TBD), bumper frame dislocated from shield structure	No complete penetration, bumper frame dislocated from shield structure	Tear on outer fabric layer, no complete penetration	No damage

DAS 2.0 NOTICE

Attention DAS 2.0 Users: an updated solar flux table is available for use with DAS 2.0. Please go to the Orbital Debris Website (<http://www.orbitaldebris.jsc.nasa.gov/mitigate/das.html>) to download the updated table and subscribe for email alerts of future updates.

THE ORBITAL DEBRIS QUARTERLY NEWS IS PUBLISHED* ON:

15 January 15 April 15 July 15 October

Visit <http://orbitaldebris.jsc.nasa.gov/newsletter/newsletter.html> to view or download ODQN issues

*When the 15th occurs on a weekend, the ODQN publishes on the following Monday

UPCOMING MEETINGS

16-18 June 2014: 3rd European Workshop on Space Debris Modeling and Remediation, Paris, France

The focus of the previous two workshops was on concepts and technology development for active debris removal of large and massive objects. The scope of the third workshop will expand to also include modeling of the future orbital debris environment, removal of millimeter and larger debris, and non-technical aspects of orbital debris environment remediation. The CNES will again organize and host this bi-annual event at its headquarters in Paris. Additional information about the event can be obtained from Dr. Christophe Bonnal at christophe.bonnal@cnes.fr.

2-10 August 2014: 40th Committee on Space Research (COSPAR) Scientific Assembly, Moscow, Russia

The main theme of the Panel on Potentially Environmentally Detrimental Activities in Space (PEDAS) for the 40th COSPAR is "Space Debris – Responding to a Dynamic Environment." The PEDAS sessions will cover areas such as advances in ground- and space-based observations and methods for their exploitation; in-situ

measurement techniques; debris and meteoroid environment models; debris flux and collision risk for space missions; on-orbit collision assessment, re-entry risk assessments, debris mitigation and debris environment remediation techniques and their effectiveness with regard to long-term environment stability; national and international debris mitigation standards and guidelines; hypervelocity accelerator technologies; and on-orbit shielding concepts. Four half-day sessions are planned. The abstract submission deadline is 14 February 2014. Additional details of the 40th COSPAR are available at: <https://www.cospar-assembly.org/>.

29 Sep - 3 Oct 2014: 65th International Astronautical Congress (IAC), Toronto, Canada

The Canadian Aeronautics and Space Institute will host the 65th IAC with a theme of "Our World Needs Space." Just like the previous IACs, the 2014 Congress will include a Space Debris Symposium to address the complete spectrum of technical issues of space debris measurements, modeling, risk assessments, reentry, hypervelocity impacts and protection, mitigation and standards, and space situational awareness. Seven sessions

have been planned to cover these topics. In addition, a joint session with the Space Security Committee on the policy, legal, and economic aspects of space debris will also be held. The deadline for abstract submission is 25 February 2014. Additional details of the Congress are available at: <http://www.iafastro.com/index.php/events/iac/iac-2014>.

20-22 Oct 2014: 7th International Association for Advancement of Space Safety (IAASS) Conference, Friedrichshafen, Germany

The 7th IAASS Conference, "Space Safety Is No Accident," is an invitation to reflect and exchange information on a number of topics in space safety and sustainability of national and international interest. The 2014 conference will dedicate a set of specialized sessions on orbital debris, including space debris remediation, reentry safety, space situational awareness and international space traffic control, and commercial human spaceflight safety. The deadline for abstract submission is 30 May 2014. Additional details of the Conference are available at: <http://iaassconference2014.space-safety.org/>

INTERNATIONAL SPACE MISSIONS

1 January 2014 – 31 March 2014

SATELLITE BOX SCORE

(as of 9 April 2014, cataloged by the
U.S. SPACE SURVEILLANCE NETWORK)

International Designator	Payloads	Country/ Organization	Perigee Altitude (KM)	Apogee Altitude (KM)	Inclination (DEG)	Earth Orbital Rocket Bodies	Other Cataloged Debris	Country/ Organization	Payloads	Rocket Bodies & Debris	Total
2014-001A	GSAT 14	INDIA	35770	35803	0.1	1	0	CHINA	158	3588	3746
2014-002A	THAICOM 6	THAILAND	35779	35794	0.1	1	0	CIS	1437	4733	6170
2014-003A	CYGNUS ORB-1	USA	402	407	51.6	1	0	ESA	47	47	94
*1998-067	(28 FLOCK 1 payloads)	USA						FRANCE	58	445	503
*1998-067EL	ARDUSAT 2	USA	392	403	51.6			INDIA	56	120	176
*1998-067EM	UAPSAT 1	PERU	364	377	51.6			JAPAN	130	81	211
*1998-067EN	SKYCUBE	USA	381	393	51.6			USA	1275	3767	5042
*1998-067EP	LITSAT 1	LITHUANIA	373	383	51.6			OTHER	623	118	741
*1998-067EQ	LITUANICASAT 1	LITHUANIA	386	397	51.6			TOTAL	3784	12899	16683
2014-004A	TDRS 12	USA	35776	35792	7.0	1	0				
2014-005A	PROGRESS M-22M	RUSSIA	411	416	51.6	1	0				
2014-006A	ABS 2	CHINA	35778	35795	0.0	1	1				
2014-006B	ATHENA-FIDUS	FRANCE/ITALY	35783	35790	0.0						
2014-007A	TURKSAT 4A	TURKEY	35773	35798	0.1	1	1				
2014-008A	NAVSTAR 69 (USA 248)	USA	20173	20192	55.0	1	0				
2014-009A	SHINDAISAT	JAPAN	370	388	65.0	1	1				
2014-009B	KSAT 2	JAPAN	351	363	65.0						
2014-009C	GPM	JAPAN	391	408	65.0						
2014-009D	OPUSAT	JAPAN	356	363	65.0						
2014-009E	TEIKYOSAT 3	JAPAN	367	380	65.0						
2014-009F	ITF 1	JAPAN	360	372	65.0						
2014-009G	INVADER	JAPAN	337	350	65.0						
2014-009H	STARS II	JAPAN	317	336	65.0						
2014-010A	EXPRESS AT1	RUSSIA	35790	35867	0.1	1	1				
2014-010B	EXPRESS AT2	RUSSIA	35781	35792	0.0						
2014-011A	AMAZONAS 4A	SPAIN	35780	35792	0.0	1	1				
2014-011B	ASTRA 5B	LUXEMBOURG	35785	35787	0.1						
2014-012A	COSMOS 2491 (GLONASS)	RUSSIA	19083	19176	64.8	1	0				
2014-013A	SOYUZ-TMA 12M	RUSSIA	413	416	51.6	1	0				
2013-014A	SJ-11-06	CHINA	687	705	98.3	1	4				

**Visit the NASA
Orbital Debris Program
Office Website**

www.orbitaldebris.jsc.nasa.gov

**Technical Editor
J.-C. Liou**

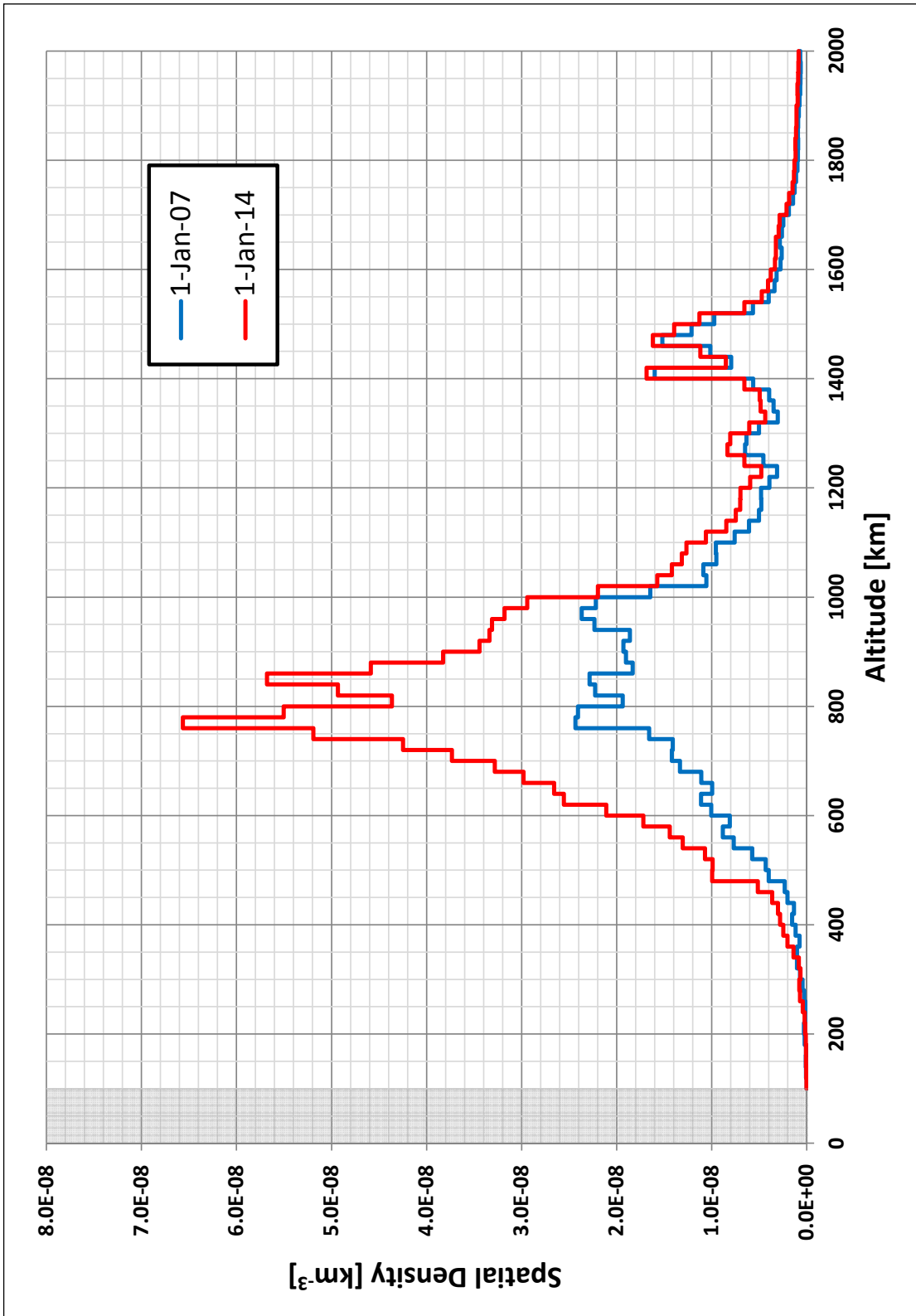
**Managing Editor
Debi Shoots**

 **Correspondence concerning
the ODQN can be sent to:**

Debi Shoots
NASA Johnson Space Center
Orbital Debris Program Office
Mail Code JE104
Houston, TX 77058

 **debra.d.shoots@nasa.gov**

*Since these satellites were ejected from the ISS, they carry the ISS International Designator.



This chart compares the spatial density distributions of the tracked objects in low Earth orbit (LEO) for 1 January 2007 and 1 January 2014. The increase below 1000 km altitude is approximately 115.4%. Fragments generated from the Fengyun-1C anti-satellite test conducted by the People's Republic of China in 2007 and the accidental collision between Iridium 33 and Cosmos 2251 in 2009 account for most of the increase.